AD-A121 027 STUDIES OF THREE-DIMENSIONAL BOUNDARY LAYERS ON BODIES OF REVOLUTION I-II..(U) DOUGLAS AIRCRAFT CO LONG BEACH CA T CEBECI ET AL. APR 82 MDC-J2506 N60921-80-C-0217 1/1

UNCLASSIFIED F/G 20/4 NL

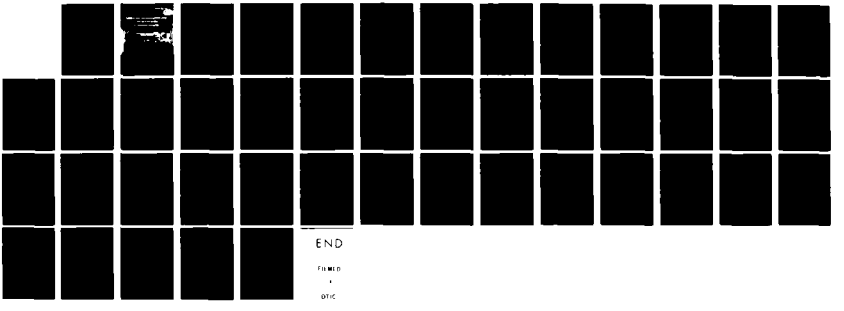

END

FILMED

DTIC

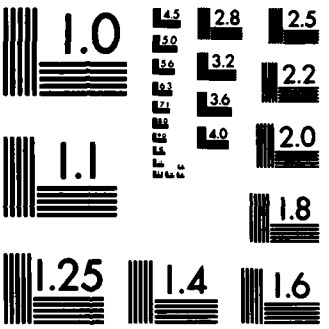

Report No. MDC J2506

STUDIES OF THREE-DIMENSIONAL BOUNDARY LAYERS ON BODIES OF REVOLUTION

III. Cones at Incidence in Supersonic Flow

by

Tuncer Cebeci, K. Kaups, A. A. Khattab
and Keith Stewartson

April 1982

Prepared under
Contract No. N60921-80-C-0217
for
Naval Air Systems Command
Washington, D.C. 20361

UNCLASSIFIED

SECURITY CLASSIFICATION OF THIS PAGE (When Data Entered)

REPORT DOCUMENTATION PAGE		READ INSTRUCTIONS BEFORE COMPLETING FORM
1. REPORT NUMBER MDC J2506	2. GOVT ACCESSION NO. AD-A121027	3. RECIPIENT'S CATALOG NUMBER
4. TITLE (and Subtitle) Studies of Three-Dimensional Boundary Layers on Bodies of Revolution. III. Cones at Incidence in Supersonic Flow		5. TYPE OF REPORT & PERIOD COVERED Final 18 Sep 1980 - 18 Sep 1981 6. PERFORMING ORG. REPORT NUMBER
7. AUTHOR(s) TUNCER CEBECI, K. KAUPS, A. A. KHATTAB, KEITH STEWARTSON		8. CONTRACT OR GRANT NUMBER(s) N60921-80-C-0217
9. PERFORMING ORGANIZATION NAME AND ADDRESS McDonnell Douglas Corporation Douglas Aircraft Company 3855 Lakewood Blvd. Long Beach, CA 90846		10. PROGRAM ELEMENT, PROJECT, TASK AREA & WORK UNIT NUMBERS 61153N; WR023-02; WR023-02-003, 2R44AA
11. CONTROLLING OFFICE NAME AND ADDRESS Naval Air Systems Command (AIR 320C) Washington, DC 20361		12. REPORT DATE April 1982 13. NUMBER OF PAGES 44
14. MONITORING AGENCY NAME & ADDRESS(if different from Controlling Office) Naval Surface Weapons Center (R44) Silver Spring, MD 20910		15. SECURITY CLASS. (of this report) UNCLASSIFIED 15a. DECLASSIFICATION/DOWNGRADING SCHEDULE

16. DISTRIBUTION STATEMENT (of this Report)

Approved for public release; distribution unlimited

17. DISTRIBUTION STATEMENT (of the abstract entered in Block 20, if different from Report)

18. SUPPLEMENTARY NOTES

19. KEY WORDS (Continue on reverse side if necessary and identify by block number)

Boundary layers
Laminar boundary layers
Boundary layer separation
Three-dimensional boundary layers
Cones

20. ABSTRACT (Continue on reverse side if necessary and identify by block number)

An investigation is carried out into the properties of a nonsimilar boundary layer on a cone at incidence with special reference to the flow near the leeside line of symmetry. The nonsimilarity is induced by allowing suction near the vertex of the cone and the external velocity is given by supersonic inviscid theory. The principal new results of the theory may be expressed in terms of a parameter -k, which is approximately equivalent to the angle of attack of the cone.

DD FORM 1 JAN 73 1473 EDITION OF 1 NOV 65 IS OBSOLETE
S/N 0102-014-6601

UNCLASSFIED

SECURITY CLASSIFICATION OF THIS PAGE (When Data Entered)

Three ranges of k have been identified. For small negative values of k, the three-dimensional boundary layer on the cone is smooth everywhere and, once the suction is removed, rapidly approaches a semi-similarity form as the distance from the vertex increases.

For more negative values of k the boundary layer is not smooth near the leeside of the cone but can be computed everywhere. The nature of this singularity is partially explained in terms of a collision phenomenon.

If k decreases further, separation occurs in computations from the windward side of the cone. The solution develops a singularity along this line provided sufficient care is taken in the calculations. An apparent nonuniqueness in the solution prevents integration from the leeside over the remainder of the region of accessibility.

SUMMARY

An investigation is carried out into the properties of a nonsimilar boundary layer on a cone at incidence with special reference to the flow near the leeside line of symmetry. The nonsimilarity is induced by allowing suction near the vertex of the cone and the external velocity is given by supersonic inviscid theory. The principal new results of the theory may be expressed in terms of a parameter -k, which is approximately equivalent to the angle of attack of the cone.

Three ranges of k have been identified. For small negative values of k, the three-dimensional boundary layer on the cone is smooth everywhere and, once the suction is removed, rapidly approaches a semi-similarity form as the distance from the vertex increases.

For more negative values of k the boundary layer is not smooth near the leeside of the cone but can be computed everywhere. The nature of this singularity is partially explained in terms of a collision phenomenon.

If k decreases further, separation occurs in computations from the windward side of the cone. The solution develops a singularity along this line provided sufficient care is taken in the calculations. An apparent nonuniqueness in the solution prevents integration from the leeside over the remainder of the region of accessibility.

CONTENTS

1.0 INTRODUCTION

In previous reports on this topic[1,2], we have reviewed progress in our study of the three-dimensional boundary layers on bodies of revolution when the external velocity is prescribed. The governing equations are parabolic in y, the coordinate normal to the body, and x, the direction of the local velocity parallel to the body, and so, were it not for two features of the problem, standard methods, which have proved to be successful in two dimensions, might readily be adapted to integrate them. The first feature, which largely formed the topic of the first report[1], is that the obvious body-based coordinate system leads to equations which contain artificial singularities. An appropriate coordinate-transformation is needed to remove them and this requires some care to devise but once it is done the coefficients of the various derivatives in the equations are bounded everywhere and they are well-adapted to standard numerical procedures.

The second feature is that the local streamwise direction in the boundary layer varies from point to point both laterally and longitudinally. Eventually as separation is approached, especially on the leeside, this gives rise to difficulties as it may be unavoidable that, over part of the boundary-layer, integration proceeds against the local flow direction., Thus it is usual to compute the solution on the windward ($\phi = 0$) and leeward ($\phi = \pi$) line of symmetries first and then at each x-station (where x measures distance along the body from the nose) integrate over the body either from $\phi = 0$ to $\phi = \pi$ or vice-versa. For such a procedure to be successful using standard methods, it is important that w (the velocity component in the ϕ direction) should not change sign as y varies for fixed x,ϕ. If it does, then whichever direction of ϕ we integrate in, over part of the range of y we must be

integrating against the local stream direction and hence not making use of all the information needed to compute the solution. In the second report[2] a remedy for this problem was devised. The numerical method in straightforward computation of boundary layers used by us is the standard box originally devised by Keller[3]. Once w changes sign, we replace it either by the zigzag box[4] or by the characteristic box[5]. Both of these methods are an improvement on the standard box in such circumstances because they take account of the extra physical information available. The zig-zag box[4] is simpler to use but is less sensitive and produces some undesirable features in the computed solution as the limit of computability is reached. The characteristic box[5] is more complicated to program but seems largely free of spurious features and is able to compute the solution practically up to the mathematical limits of the formulation.

This limit is the accessibility boundary and there are precise mathematical reasons why the computation cannot be extended beyond it. Partly it consists of the separation line, at which the solution develops a singularity and partly by an external streamline passing through the forward separation point A, known as the ok (Turk. arrow) of accessibility. The situation is illustrated in Fig. 1.

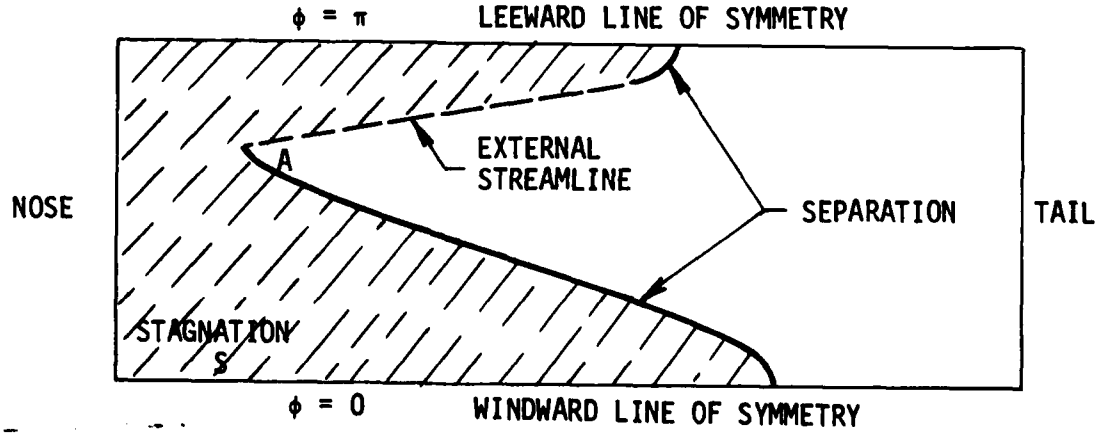

Fig. 1. The solution can be computed over the hatched part of the body starting from the forward stagnation point. Notice that the nose and tails are single points but in polar coordinates they must be replaced by lines ($0 \leq \phi \leq \pi$).

Future work envisaged at the completion of these studies was to interact the boundary-layer computation with an inviscid code which would thereupon remove the barrier imposed by the singularity at separation and enable us to compute the flow field over the whole body. We also wished to study other body shapes to investigate how far the conclusions from this work could be regarded as general.

The first part of such work is a large program of study and has proceeded independently of the work to be described in this report but it is useful to comment briefly on what has been achieved. Interactive studies have been completed on two problems in two-dimensional flow[6,7]. We have examined the boundary layer near the leading edge of a thin airfoil at incidence[6,7] and shown that once interaction with the external stream is permitted, the existence of separation no longer prevents the successful completion of the solution. Comparison with experimental data obtained by Gault[8] is generally favorable[9]. However, there is a curious feature of the solution which appears to be a genuine property of high-Reynolds number flows. This is that although reversed flow can be found but its extent is limited before the whole iteration procedure fails to converge. A mathematical analysis of the solution[7] confirms the correctness of the general conclusion and it is also broadly unaltered if transition to a turbulent boundary layer occurs, the turbulence being modelled by an algebraic eddy viscosity. It appears that the notion of a thin boundary layer on the airfoil modifying an external potential flow has a certain range of validity in which is included the occurrence of a small region of reversed flow in the boundary layer, but thereafter becomes inappropriate. One may crudely regard the approach as going sour. In view of this, it was decided to carry out a further comparison, with Briley's solution, using the Navier-Stokes equations of a problem with separation[10].

Again good agreement was obtained with his published data and again the boundary-layer approach eventually went sour. In the same conditions, Briley's numerical procedure failed to converge. Although he attributed this to a physical instability of the flow, we have reservations and believe that dramatic changes are occurring in the solution for which his domain of integration is too small to describe adequately. Work is in progress to explore this problem further.

The subject of this report is the progress made in applying boundary-layer theory, without interaction, to the computation of supersonic flow past cones at incidence. In its simplest form this is a two-dimensional problem because the streamwise coordinate can be absorbed in the formulation and the independent variables are η, the reduced normal distance from the cone and ϕ, the azimuthal angle measured from the windward line of symmetry. Solutions can always be found at $\phi = 0$ and continued round towards $\phi = \pi$, the leeward line of symmetry, but are difficult to find near $\phi = \pi$ even if separation does not occur beforehand. At $\phi = \pi$ pairs of solutions can be found in certain circumstances but none in others and the situation is not always compatible with the solution properties for $\phi < \pi$. One aim of this report is to reconcile these features of the flow.

Commonly, cones do not occur alone in practical configurations but are part of more complicated shapes having attached to them fins and afterbodies, which may be boattailed and asymmetric, and possibly rounded noses. It was thought appropriate, therefore, to set the semi-similar solutions, described above, in a more general context and with this in mind we introduced suction near the vertex of the cone so that a self-similar solution is only generated at some distance along it. We expect that if separation occurs, there would also exist an accessibility boundary and we should be able to investigate its properties. Looking further ahead, we shall then be able to comment on the

parabolic elliptic boundary layer (PEBL) method of computing the boundary layer once separation has occurred. We have reservations about this method since there is a nonphysical basis to it. Another, more promising, method is the use of parabolized Navier-Stokes equations[11,12] and we expect that the extension of our work to include interaction will lead to a useful alternative way of tackling practical problems and have a status similar to that in the two-dimensional flows discussed earlier.

2.0 GOVERNING EQUATIONS

The governing boundary-layer equations for compressible laminar and turbulent flows on a general conical surface of semi-vertex angle β_c are well known and can be written in the following form:

Continuity:

$$\frac{\partial}{\partial x}(\rho u x) + \frac{\partial}{\partial \theta}(\rho w) + \frac{\partial}{\partial y}(\overline{\rho v} x) = 0 \tag{2.1}$$

x-Momentum

$$\rho u \frac{\partial u}{\partial x} + \rho \frac{w}{x}\frac{\partial u}{\partial \theta} + \overline{\rho v}\frac{\partial u}{\partial y} - \rho \frac{w^2}{x} = \frac{\partial}{\partial y}\left(\mu \frac{\partial u}{\partial y} - \rho\overline{u'v'}\right) \tag{2.2}$$

θ-Momentum

$$\rho u \frac{\partial w}{\partial x} + \rho \frac{w}{x}\frac{\partial w}{\partial \theta} + \overline{\rho v}\frac{\partial w}{\partial y} + \rho \frac{uw}{x} = -\frac{1}{x}\frac{dp}{d\theta} + \frac{\partial}{\partial y}\left(\mu \frac{\partial w}{\partial y} - \rho\overline{w'v'}\right) \tag{2.3}$$

Energy

$$\rho u \frac{\partial H}{\partial x} + \frac{\rho w}{x}\frac{\partial H}{\partial \theta} + \overline{\rho v}\frac{\partial H}{\partial y} = \frac{\partial}{\partial y}\left[\frac{\mu}{Pr}\frac{\partial H}{\partial y} + \mu\left(1 - \frac{1}{Pr}\right)\frac{\partial}{\partial y}\left(\frac{u^2 + w^2}{2}\right) - \rho\overline{v'H'}\right] \tag{2.4}$$

Here $\overline{\rho v} = \rho v + \overline{\rho' v'}$; θ denotes the polar coordinate in the developed plane; x the coordinate along the generators; and y the coordinate normal to the surface; with w, u, v the velocities in the θ, x and y directions.

At the windward and leeward stagnation lines where $\theta = 0$ and $\pi \sin\beta_c$, the cross-flow momentum equation is an identity since $w \equiv dp/d\theta \equiv 0$. Taking into account the symmetry conditions and differentiating Eq. (2.3) with respect to θ, we can write it as

$$\rho u \frac{\partial w_\theta}{\partial x} + \rho \frac{w_\theta^2}{x} + \overline{\rho v} \frac{\partial w_\theta}{\partial y} + \rho \frac{u w_\theta}{x} = -\frac{1}{\rho} \frac{d^2 p}{d\theta^2} + \frac{\partial}{\partial y} \left[\mu \frac{\partial w_\theta}{\partial y} - \rho (\overline{w' v'})_\theta \right] \tag{2.5}$$

where $w_\theta = \partial w / \partial \theta$. Noting that $w = 0$, Eqs. (2.1), (2.2) and (2.4) can be simplified and written as

$$\frac{\partial}{\partial x} (\rho u x) + \rho w_\theta + \frac{\partial}{\partial y} (\overline{\rho v} x) = 0 \tag{2.6}$$

$$\rho u \frac{\partial u}{\partial x} + \overline{\rho v} \frac{\partial u}{\partial y} = \frac{\partial}{\partial y} (\mu \frac{\partial u}{\partial y} - \rho \overline{u' v'}) \tag{2.7}$$

$$\rho u \frac{\partial H}{\partial x} + \overline{\rho v} \frac{\partial H}{\partial y} = \frac{\partial}{\partial y} \left[\frac{\mu}{Pr} \frac{\partial H}{\partial y} + \mu \left(1 - \frac{1}{Pr}\right) \frac{\partial}{\partial y} \left(\frac{u^2}{2}\right) - \rho \overline{v' H'} \right] \tag{2.8}$$

Before we discuss the solution of the above equations, we express them in terms of similarity variables. For the general case in which the governing equations are given by those defined by Eqs. (2.1) to (2.4), we define

$$d\eta = \left(\frac{u_e}{\rho_e \mu_e x}\right)^{1/2} \rho dy \tag{2.9}$$

In addition, we introduce a two-component vector potential such that

$$\rho u x = \frac{\partial \psi}{\partial y}, \qquad \rho w x = \frac{\partial \phi}{\partial y}, \qquad \overline{\rho v} x = -\frac{\partial \psi}{\partial x} - \frac{1}{x} \frac{\partial \phi}{\partial \theta} + x(\rho v)_w \tag{2.10}$$

and dimensionless functions ψ and Φ

$$\psi = (\rho_e \mu_e u_e)^{1/2} x^{3/2} f(x,\theta,\eta) \tag{2.11a}$$

$$\Phi = (\rho_e \mu_e u_e)^{1/2} x^{1/2} g(x,\theta,\eta) \tag{2.11b}$$

Using these transformations and the eddy viscosity and turbulent Prandtl number concepts, that is,

$$-\rho\overline{u'v'} = \rho\varepsilon_m \frac{\partial u}{\partial y}, \quad -\rho\overline{w'v'} = \rho\varepsilon_m \frac{\partial w}{\partial y}, \quad -\rho\overline{v'H'} = \sqrt{2}\,\frac{\varepsilon_m}{Pr_t}\frac{\partial H}{\partial y} \tag{2.12}$$

We can write Eqs. (2.1) to (2.4) as

$$(bf'')' + \frac{3}{2} ff'' - \left(\frac{w_e}{u_e}\right) f'g' + (g')^2 + mf''g + \frac{w_e}{u_e} g'f'' + Pf''$$
$$= x\left(f' \frac{\partial f'}{\partial x} - f'' \frac{\partial f}{\partial x}\right) + g' \frac{\partial f'}{\partial \theta} - f'' \frac{\partial g}{\partial \theta} \tag{2.13}$$

$$(bg'')' + \frac{3}{2} fg'' - f'g' + mgg'' + \frac{w_e}{u_e}(g'g'' - g'^2) + \frac{\rho_e}{\rho}\frac{w_e}{u_e}\left(1 + \frac{1}{u_e}\frac{\partial w_\theta}{\partial \theta}\right) + Pg''$$
$$= x\left(f' \frac{\partial g'}{\partial x} - f'' \frac{\partial g}{\partial x}\right) + g' \frac{\partial g'}{\partial \theta} - g'' \frac{\partial g}{\partial \theta} \tag{2.14}$$

$$\left[b_1 E' + C \frac{u_e^2}{H_e}\left(1 - \frac{1}{Pr}\right) f'f'' + g'g''\right]' + \frac{3}{2} fE' + mgE' + PE'$$
$$= x\left(f' \frac{\partial E}{\partial x} - E' \frac{\partial f}{\partial x}\right) + g' \frac{\partial E}{\partial \theta} - E' \frac{\partial g}{\partial \theta} \tag{2.15}$$

Here primes denote differentiation with respect to η and

$$f' = \frac{u}{u_e}, \qquad g' = \frac{w}{u_e}, \qquad E = \frac{H}{H_e}, \qquad b = C(1 + \varepsilon_m^+)$$

$$\varepsilon_m^+ = \frac{\varepsilon_m}{\nu}, \qquad C = \frac{\rho\mu}{\rho_e\mu_e}, \qquad b_1 = \frac{C}{Pr}\left(1 + \sqrt{2}\,\varepsilon_m^+ \frac{Pr}{Pr_t}\right) \tag{2.16}$$

$$m = \frac{1}{2}\left[-\frac{w_e}{u_e} + \frac{1}{(\rho\mu)_e}\frac{d(\rho\mu)_e}{d\theta}\right], \qquad P = -\frac{(\rho v)_w}{\rho_e u_e} R_x^{1/2}$$

Similarly the line-of-symmetry equations, Eqs. (2.5) to (2.8) can be transformed and expressed in a form similar to those given by Eqs. (2.13) to (2.15) by using the transformations given by Eqs. (2.9) to (2.11) with slight modification to the following parameters

$$\rho w_\theta = \frac{\partial \Phi}{\partial y}, \qquad \overline{\rho v x} = -\frac{\partial \psi}{\partial x} - \Phi + (\rho v)_w x \tag{2.17}$$

$$\psi = (\rho_e \mu_e x)^{3/2} F(x,\eta) \tag{2.18a}$$

$$\phi = (\rho_e \mu_e x)^{1/2} G(x,\eta) \tag{2.18b}$$

Equations (2.5), (2.7) and (2.8) then become

$$(bF'')' + \left(\frac{3}{2}F + G + P\right)F'' = x\left(F'\frac{\partial F'}{\partial x} - F''\frac{\partial F}{\partial x}\right) \tag{2.19}$$

$$(bG'')' + \left(\frac{3}{2}F + G\right)G'' - G'^2 - F'G' + \frac{1}{u_e}\frac{dw_e}{d\theta}\left(1 + \frac{1}{u_e}\frac{dw_e}{d\theta}\right)\frac{\rho_e}{\rho} + PG''$$
$$= x\left(F'\frac{\partial G'}{\partial x} - G''\frac{\partial F}{\partial x}\right) \tag{2.20}$$

$$\left[b_1 E' + \frac{Cu_e^2}{H_e}\left(1 - \frac{1}{Pr}\right) F'F''\right]' + \left(\frac{3}{2}F + G + P\right)E' = x\left(F' \frac{\partial E}{\partial x} - E' \frac{\partial F}{\partial x}\right) \qquad (2.21)$$

Here $G' = w_\theta / u_e$.

The boundary conditions are

$$f' = g' = g = F' = \mathcal{G}' = G = 0 \qquad \text{at} \qquad \eta = 0 \qquad (2.22)$$

and

$$f' = E = F' = 1, \qquad g' = G' = \frac{1}{u_e}\frac{dw_e}{d\theta} \qquad \text{at} \qquad \eta = \infty$$

In addition either E' or E may be prescribed at $\eta = 0$ and in order to start the computations we shall apply suction to the boundary layer in $0 \leq x \leq 0.05$. Thus f is a prescribed function of θ when $\eta = 0$ for these values of x and thereafter $f = 0$ at the wall. It is convenient to introduce a parameter k in the line-of-symmetry studies defined by Moore[13] to be

$$k = + \frac{2}{3}\frac{dw_e}{d\theta}\frac{1}{u_e} \qquad (2.23)$$

The explicit forms for u_e and w_e follow from inviscid conical flow theory and are

$$u_e = 1 + A \sin\beta_c - A \sin\beta_c \cos(\theta/\sin\beta_c), \quad w_e = A \sin(\theta/\sin\beta_c) \qquad (2.24)$$

where β_c is the semi-vertex angle of the cone and A is a constant depending on β_c, M_∞ and α, the angle of attack of the cone. Typically $A \sim 1/4$ and explicit values have been tabulated by Sims[14]. The numerical calculations

to be described in Sec. 3 were carried out for $\beta_c = 10^o$. It will be convenient subsequently to define $\phi = \theta/\sin\beta_e$, to be the angular distance around the cone from the windward line of symmetry so that $\phi = \pi$ is the leeward line of symmetry.

Since the studies are basic in nature, there is no advantage in solving the governing equations for a general fluid. Consequently we set

$$Pr = 1 \qquad \text{and} \qquad \mu\rho = \mu_e\rho_e, \qquad \text{i.e.} \qquad C = 1 \tag{2.25}$$

A further simplification is to assume that the thermal boundary condition is either that cone is adiabatic or the wall temperature is prescribed. Then (2.15) reduces to

$$E = E_w(1 - S) + S \tag{2.26}$$

where $S = 1$ or F', respectively, for the two cases. Hence

$$\frac{\rho_e}{\rho} = (1 + \tfrac{1}{2}(\gamma - 1)M_e^2)(S + E_w(1 - S)) - \tfrac{1}{2}(\gamma - 1)M_e^2F'^2 \tag{2.27}$$

3.0 RESULTS

We have used the box method to solve the governing equations discussed in the previous section. In regions where the circumferential velocity component changed sign becoming negative, we used the zig-zag box method. Since both of these methods are already discussed in detail in several references[2,4,15], we shall not elaborate them here but only present the results of the computations.

3.1 The Leeside Line of Symmetry in Laminar Flow

Since we have an extensive body of new results for this aspect of the flow field, it is worthwhile to begin our discussion of them with a review of previous work.

The boundary-layer equations appropriate to the windward and leeward lines of symmetry of a cone fixed in a supersonic external stream were first written down by Moore[13] in terms of a parameter k (positive for the windward line of symmetry and negative for the leeward, defined in (2.23)). The value of k, for a prescribed external Mach number and ratio of wall to freestream enthalpy, determines the existence or otherwise of a solution of these similarity equations. The solution of these equations in our independent variable exist for all $k < 0$ and for certain $k > 0$ though they may not be unique. They are expected to be solutions of the full boundary-layer equations in the limit $x \to \infty$ where x measures distance along a generator, and as $\phi \to 0$ or π where $\phi = 0$ is the windward plane of symmetry and $\phi = \pi$ the leeward. These equations have been considered by Cheng[16], Roux[17], Murdock[18], Wu and Libby[19] and Rubin, Line and Tarulli[20].

One way of attempting to gain an understanding of the nonuniqueness and nonexistence of these similarity solutions is to explore the independent variable x and to integrate the nonsimilar equations for the symmetry planes along the generator with increasing distance from the vertex as was undertaken for example by Rubin et al[20]. The solution so found either breaks down at a finite value of x, or it may be continued to $x = \infty$ the limit solution possibly being given by the similarity equations. Another way is to restore ϕ rather than x and to perform a windward to leeward integration in the manner of Cooke[21], Boericke[22], Roux[17], and Tarulli[23]. If $\phi = \pi$ is attained then the limit solution may or may not be a solution of the similarity equations. A third approach is to solve the complete equations in the manner of Boericke[22] and Dwyer[24]. Since there are three parameters involved and the similarity equations have nonunique solutions, a complete documentation of the relation behavior the various approaches has not yet been achieved.

One of the aims of the present investigation is to examine the possibility that the solution of the nonsimilar equations for the leeward plane of symmetry comes to an end at a finite value of x. Rubin et al.[20] noted that for those k for which they encountered this phenomenon, the streamwise skin friction vanished though this did not seem to be a separation of the Goldstein type in that it was caused not by an adverse pressure gradient but by a violation of the assumption that the crossflow is zero on the plane of symmetry. The crossflow boundary layers were colliding and forcing the streamwise boundary layer to leave the wall. The situation is very similar to that encountered by Stewartson, Cebeci and Chang[25] in their study of the development of a laminar boundary layer near the entrance of a loosely coiled pipe. On the inner line of symmetry there appeared to be a local singularity where the axial component of skin friction vanished. Further downstream, the flow was

well-behaved except in the immediate neighborhood of the inner generator. The two secondary boundary layers had collided. The behavior of the solution near the local singularity has more recently been analyzed by Stewartson and Simpson[26] and our aim in this study is to demonstrate that their analysis is also applicable to the colliding boundary layers on the leeward side of the cone.

We shall show that a singularity is theoretically possible if $0 > k > -2/3$, regardless of the Mach number M_e and enthalpy ratio E_w, and, further, that much of the analysis of ref. 26 may be taken over without revision although there are significant differences in the outer part of the terminal boundary layer. Similarity solutions are possible in two ranges of values of k and then, most probably, occur in pairs. The first range is $k > k_1^*$ where $k_1^* > -2/3$ is a number depending on the Mach number M_e and the enthalpy ratio E_w. Thus, if $M_e = 0$ we have found numerically that $k_1^* = -0.292$ but no attempt was made to find any dual solutions in $k > k_1^*$. The existence of the second solution was established by Murdock[18] in computations with $E_w = 0.4$, and $M_e^2 = 16/(\gamma - 1)$, when $k_1^* = -0.079$. A second range of k for which similarity solutions are possible is $k_2^* > k > -1$ where k_2^* is very close to -2/3 but distinct from it. Thus Murdock gives $k_2^* = -0.6656$. If $M_e = 0$ we were unable to find a similarity solution when $k = -0.66$ and when $k = -2/3$ there are at least two solutions for all M_e, E_w[13,18].

Numerical solutions of the nonsimilarity leeside equations are found here for a number of values of k and $M_e = 0$, it being considered that the character of the solutions is independent of M_e, E_w. If $k = -0.25$ the solution may be found for all distances x along the leeside generator and it approaches the primary similarity solution as $x \to \infty$, and this is also the limit of the

corresponding equations in which the x-variation is suppressed and ϕ allowed to increase from $\phi = 0$ at the windward line of symmetry to $\phi = \pi$. If $k = -0.5$, the solution terminated at a finite value of x in a singularity in accord with our theoretical considerations. If $k = -0.70$ it appears that the solution may be continued indefinitely in x. We infer that a singularity will occur if $k_1^* > k > k_2^*$.

3.2 Numerical Studies

Equations (2.19) to (2.21) hold for either the windward or leeward planes of symmetry. At the windward plane of symmetry $k > 0$ and at the leeward plane $k < 0$. There are three nondimensional parameters in the problem, namely M_e, k and E_w, and both the nonsimilar and similar forms of (2.19) to (2.21) have been considered by various authors. A useful summary of earlier work is given by Rubin, Lin and Tarulli[20]. Dual similarity solutions exist for $k > k_1^*$ and again when $-1 < k < k_2^*$ where $k_2^* \beta k_1^* < 0$ and k_1^*, k_2^* depend on the values of M_e and E_w (see refs. 16 to 19). When $k_1^* > k > k_2^*$ no solutions of the similarity equations exist and solutions by Cooke[21], Boericke[22], among others, from the windward plane of symmetry to the leeward plane of symmetry of the equations for the cone with the ϕ dependence retained but with $x = \infty$ indicate that, for such k, the assumption implicit in (2.19) to (2.21) that the azimuthal velocity is proportional to $\pi - \phi$ is invalid. Rather it remains nonzero as $\phi \to \pi$ with the result that the boundary layers growing on either side of the cone will collide. Integration of (2.19), (2.20) for certain k in this range by Rubin et al.[20] demonstrates the existence of a point x_s at which the streamwise component of skin friction (u_y at $y = 0$) vanishes. As the incidence is increased so that k is less than k_2^* it is likely that there is cross-flow reversal in the windward to leeward integration before ϕ reaches π.

It is the collision phenomenon and the existence of the "separation" point x_s of Rubin et al.[20] that interests us here. As this appears regardless of the values of M_e and E_w we set $M_e = 0$ and $E_w = 1$ in (2.19) to (2.21) and found solutions of these equations and of the equations considered by Boericke and Dwyer[24] for negative values of k. The integration of the leeside equations is initiated by assuming that the cone is permeable in $0 \leq x \leq 0.05$ and that $F(P) > 0$ in this range, but $F(P) \to 0$ as $x \to 0.05$. The precise form of P is given in (3.26) below. The initial profile is then computed at $x = 0$, evolves as x increases, and either terminates at a finite value of x in a collision or may be continued to $x = \infty$. The only noteworthy characteristic of the solution is that the boundary-layer thickness increases rapidly near any breakdown point but it was then only found necessary to increase the number of points across the boundary layer. The step length in η is 0.1 and that in x is in the range 0.0015 to 0.025, consistent with accuracy. The numerical method was also used to solve the similarity equations ((2.19) with $\partial/\partial x = 0$) and also the windward-leeward equations the step length in ϕ, where $\phi \sin\beta_c = \theta$, varying from 5° near $\phi = 0$ to as little as 0.1° near $\phi = 180°$.

The results are in general agreement with those of previous workers. For the similarity equation we find that $k_1^* = -0.292$ and $k_2^* = -0.666$. In Fig. 2a we display the wall shear parameter F''_w computed from the similarity equations and from the ϕ-wise integration. In the range $k_1^* < k < 0$ the primary similarity solution is also the limit solution of the ϕ-integration. For $k_1^* > k > k_3^*$ where $k_3^* \simeq -0.80$, the ϕ-integration leads to a collision at $\phi = 180°$ as can also be seen from Fig. 2b in which we plot the value of $(\pi - \phi)G''_w$ in the limit $\phi = \pi$. The similarity solutions for $k < k_2^*$ do not appear to be relevant to the ϕ-integration solutions. For $k < k_3^*$

separation occurs before the leeside is reached. In Fig. 3 we display the results of the leeside integrations. For $k = -0.25$ the solution appears to exist for all x and to approach the primary similarity solution as $x \to \infty$. For $k = -0.50$ the solution exhibits the "separation" point x_s with $F_w'' = 0$. For $k = -0.65, -0.66$ no initial solutions could be found for any values of $P_0 = 3/2\ F(0,0)$. For $k = -0.70$ the solution can apparently be continued for all x, and approaches one of the similarity solutions as $x \to \infty$ is $P_0 \leq 0.40$. The fate of the solution with $P_0 = 0.70$ as $x \to \infty$ is not clear.

We shall not adopt the term separation for the point x_s as it is not the usual Goldstein form but is reminiscent of the heralding of the collision of the boundary layers on the line of symmetry of a curved pipe recently studied by Stewartson, Cebeci and Chang[25] and by Stewartson and Simpson[26]. In the latter paper the authors showed that the streamwise skin friction vanishes with a singularity that is not of the Goldstein type, but is weaker, and signals a lifting of the streamwise boundary layer from the wall as the crossflow boundary layers presumably collide underneath it. They present an analysis which agrees well with their numerical study. We now show that if $0 > k > -2/3$, the same analysis may be applied to equations (2.19) - (2.21) with encouraging agreement with a representative computation carried out when $k = -0.5$ and $M_e = 0$, $E_w = 1$, the incompressible case.

3.3 The Singularity at the Start of Collision on the Leeward Side of Symmetry

The theory of ref. 26 for the curved pipe may be applied directly to the system (2.19) - (2.21) for all M_e and E_w provided $3/2\ k^2 + k > 0$. In ref. 26 the authors assume the existence of a point $x = x_s$ at which the

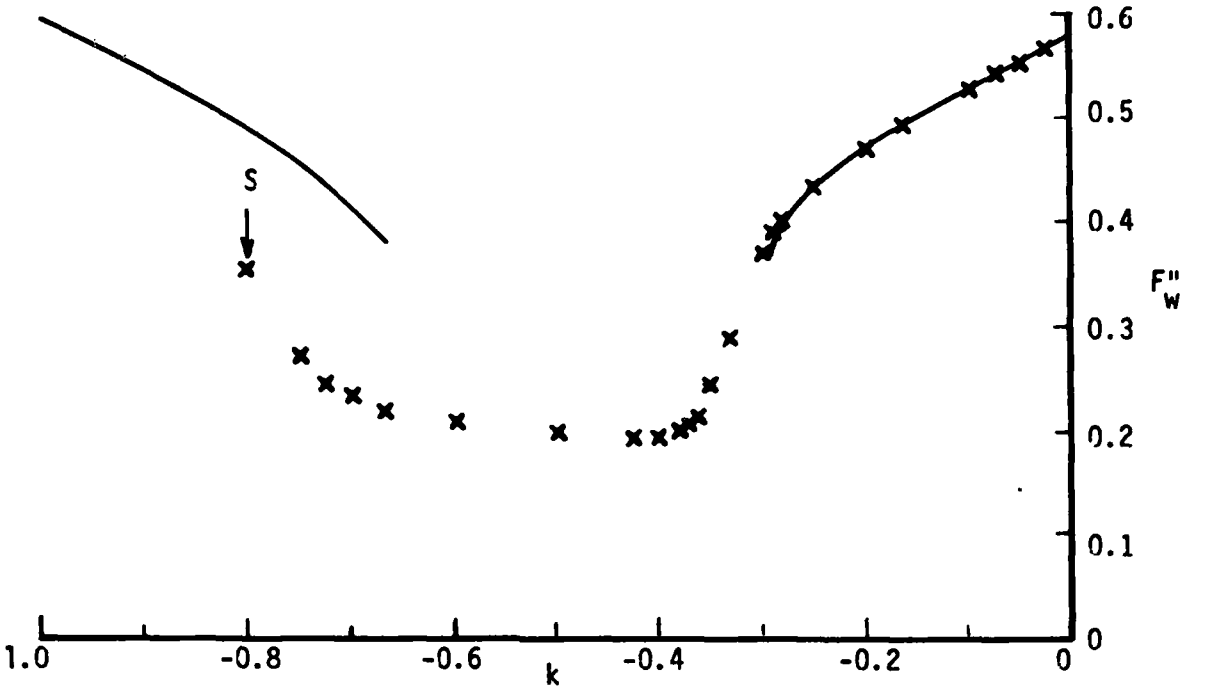

Fig. 2a. The wall shear parameter F''_w from the similarity equations (continuous curve) and the ϕ-wise integration (crosses). S denotes the onset of separation of the crossflow before ϕ reached π.

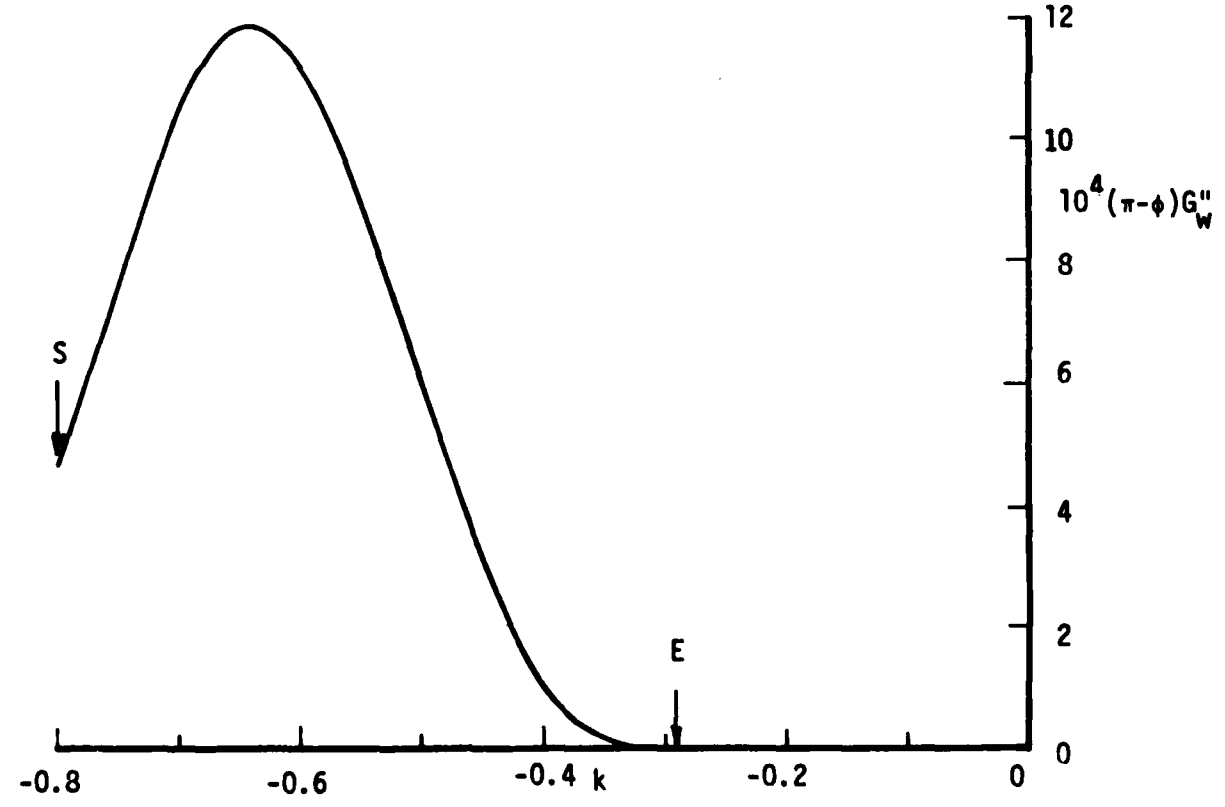

Fig. 2b. The values of $10^4\ (\pi - \phi)G''_w$ as $\phi \to \pi$ in the ϕ-wise integration. S denotes the onset of separation of the crossflow for $\phi < \pi$ and E denotes $k = k_1$, where the similarity solution comes to and end.

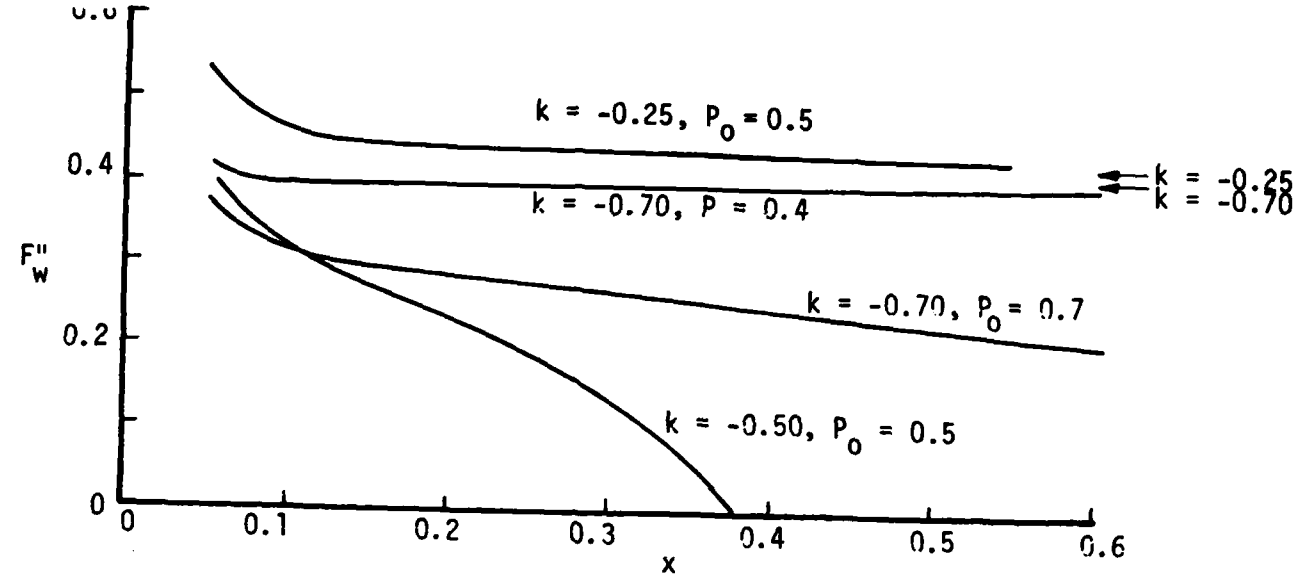

Fig. 3a. The values of F''_w from the leeside integration. The arrows indicate the similarity limits for k = -0.25 and k = -0.70. The plot starts at x = 0.05 where the suction was terminated.

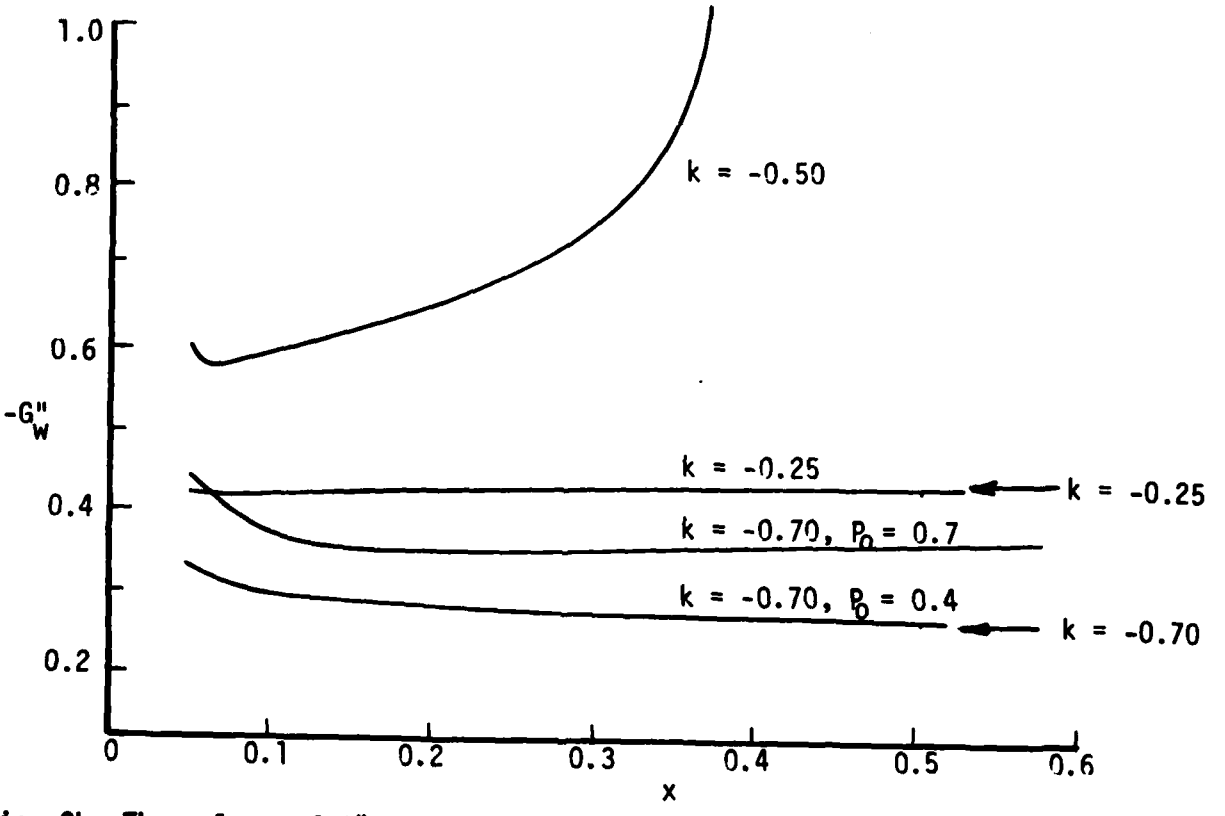

Fig. 3b. The values of G''_w from the leeside integration. The arrows indicate the similarity limits for k = -0.25 and k = -0.70. The plot starts at x = 0.05 where the suction was terminated.

streamwise skin friction, F''_w, vanishes and show that a consistent structure may be obtained in its neighborhood. In order to facilitate comparison with their work we first define

$$x = e^X, \quad \eta = K^{-1/4}Y, \quad F' = K^{1/2}U, \quad G' = K^{1/2}W, \quad -\frac{3}{2}F + G - x\frac{\partial F}{\partial x} = K^{1/4}V \tag{3.1}$$

where K is a positive constant which later on we shall choose to be

$$-\frac{3}{2}k\left(\frac{3}{2}k + 1\right)\rho_e/\rho_w$$

where ρ_w is the value of ρ on the wall. Then equations (2.19) may be replaced by

$$U\frac{\partial U}{\partial X} + V\frac{\partial U}{\partial Y} = \frac{\partial^2 U}{\partial Y^2} \tag{3.2a}$$

$$U\frac{\partial W}{\partial X} + V\frac{\partial W}{\partial Y} + UW - W^2 + \frac{3}{2}\frac{k}{K}\left(\frac{3}{2}k + 1\right)\frac{\rho_e}{\rho} = \frac{\partial^2 W}{\partial Y^2} \tag{3.2b}$$

$$\frac{\partial U}{\partial X} + \frac{\partial V}{\partial Y} + \frac{3}{2}U - W = 0 \tag{3.2c}$$

Also (2.22), (2.23) become

$$U = V = W = 0 \quad \text{on} \quad Y = 0 \tag{3.3}$$

$$U \to K^{-1/2}, \quad W \to -3/2\ kK^{-1/2} \quad \text{as} \quad Y \to \pi \tag{3.4}$$

together with

$$\frac{\rho_e}{\rho} = \left[1 + \frac{1}{2}(\gamma - 1)M_e^2\right]\left[S + E_w(1 - S)\right] - \frac{1}{2}(\gamma - 1)M_e^2 KU^2 \tag{3.5}$$

where $S = 1$ if the wall is adiabatic, and $S = K^{1/2}U$ if the wall temperature is prescribed. In the above, U is simply a scaled velocity component along

the leeward line of symmetry, W a scaled azimuthal velocity component with the factor $\pi - \phi$ removed, and V is related to the normal velocity.

In ref. 26 the authors showed that the flow in the neighborhood of the singularity required analysis in three different regions. In the inner region $U \alpha (X_s - X)$ and is negligible in (3.2), (3.5) except where the term also contains the derivative with respect to X as these are assumed to be large. Thus to leading order in $X_s - X$ we may ignore the term UW in (3.2b), the term 3/2 U in (3.2c) and (3.5) becomes $\rho = \rho_w$. We now choose $K = -3/2\ k\ (3/2\ k + 1)\rho_e/\rho_w$ and then in the inner layer the equations are exactly those that hold in the neighborhood of the inner generator of the curved pipe of ref. 26 when terms of relative order $X_s - X$ are neglected. Then, as there, the solution in the inner layer is of the form

$$U = \mu_1^{2/3}(X_s - X)\{\eta_1 + \sum_{n=1}^{\infty} \mu_1^{-4n/3} U_n(\eta_1)\} + O\{(X_s - X)^2\},$$

$$V = \mu_1^{1/3}\{\eta_1^2 + \sum_{n=1}^{\infty} \mu_1^{-4n/3} V_n(\eta_1)\} + O(X_s - X) \qquad (3.6)$$

$$W = \mu_1^{2/3}\{\eta_1 + \sum_{n=1}^{\infty} \mu_1^{-4n/3} W_n(\eta_1)\} + O(X_s - X)$$

the only difference, apart from the different usage for the symbols U, V, W, (U, V, W of ref. 26 correspond to V, W, U here), being the order of the error terms in (3.6). In the above $\mu_1 >> 1$ and

$$\eta_1 = Y\mu_1^{1/3}, \quad \mu_1^{4/3} - \alpha_1\alpha_2 \log(\mu_1^{4/3} + \alpha_1\alpha_2) = \frac{4\alpha_1}{3} \log \frac{\beta_1}{X_s - X} \qquad (3.7)$$

where $\alpha_1 = 0.5325$, $\alpha_2 = -0.4636$ are constants determined by the singularity itself and β_1 is a constant that depends on the previous history of the

flow for $X < X_s$. In ref. 26 terms of (3.6) up to n = 2 were explicitly calculated, and they are exactly the same in this case. All we shall require here in detail is the behavior of U and W of (3.6) when $\eta_1 >> 1$ as this is needed for a match with the outer solution. These are obtained directly from (4.11) of ref. 26 as

$$\begin{aligned} U &\sim (X_s - X)\mu_1^{2/3}[\eta_1 - \mu_1^{-4/3}\{-\tfrac{1}{4}\eta_1^2 + \alpha_1\eta_1 \log\eta_1 + O(\eta)\} \\ &\qquad + \mu_1^{-8/3}\{\tfrac{1}{24}\eta_1^3 + O(\eta_1^2)\} + \ldots] \\ W &\sim \mu_1^{2/3}[\eta_1 - \mu_1^{-4/3}\{\tfrac{1}{4}\eta_1^2 + \alpha_1\eta_1 \log\eta_1 + O(\eta_1)\} \\ &\qquad + \mu_1^{-8/3}\{\tfrac{1}{24}\eta_1^3 + O(\eta_1^2)\} + \ldots] \end{aligned} \tag{3.8}$$

In ref. 26 there is assumed to be an inviscid region between the wall layer discussed above and the main part of the streamwise boundary layer which has been forced away from the wall by the colliding crossflow boundary layers. There is an analogous, though not identical, solution to equations (3.2) in this situation. We neglect the viscous terms and note that ρ_e/ρ is no longer a constant in this region but is given by (3.5) though we take the same value for K as defined above. If V is eliminated between the inviscid forms of (3.2a), (3.2b) and $3/2\ k(3/2\ k + 1)\rho_e/(\rho K)$ is denoted by -R(U), then they may be solved for W in terms of U to give

$$\frac{W - 1/2\ U}{[R(U) - 1/4\ U^2]^{1/2}} = \cot\left\{\frac{[X_s - X + f_1(U)][R(U) - 1/4\ U^2]^{1/2}}{U}\right\} \tag{3.9}$$

when $R(U) > 1/4\ U^2$ which holds near the wall where $U \simeq 0$ and $R(U) \simeq 1$, but

$$\frac{W - 1/2\ U}{[1/4\ U^2 - R(U)]^{1/2}} = \coth\left\{\frac{[X_s - X + f_1(U)][1/4\ U^2 - R(U)]^{1/2}}{U}\right\} \tag{3.10}$$

when $R(U) = 1/4U^2$ which holds as $Y \to \infty$ where $1/4U^2 - R(U) = 1/4K\,(3k + 1)^2$. Here $f_1(U)$ is an arbitrary function of U, and U is assumed to vary monotonically from its value 0 at the wall to $K^{-1/2}$ as $Y \to \infty$. The solutions (3.9), (3.10) continue smoothly through the zero of $R(U) - 1/4\,U^2$. At $Y = \infty$, $(W - 1/2\,U)(1/4\,U^2 - R(U))^{-1/2} = -(3k + 1)/|3k + 1|$ so is negative if $k > -1/3$ and if the inviscid solution is to satisfy the boundary condition then the right-hand side of (3.10) must tend to -1 as U tends to $K^{-1/2}$. This means that $f_1(U) \to -\infty$ as $U \to K^{-1/2}$ but, as shown below, $f_1(U) > 0$ as $U \to 0$ so $f_1(U)$ must vanish for some $U > 0$. As the wall layer is approached W is large and positive while U is proportional to $X_s - X$ and is thus negligible. Thus, if $k > 1/3$, $W - 1/2\,U$ has to change sign and this will occur in the region where (3.9) holds as the hyperbolic cotangent cannot vanish. It is not clear in which region $f_1(U)$ will vanish for nonzero U. This zero of $f_1(U)$ in addition to that which occurs when $U = 0$ will imply that W is again very large and could lead to an additional singularity; this time in the interior of the fluid, but further numerical work is required to verify this. Our prototype solution is at $k = -1/2$ which is in the range $-2/3 < k < -1/3$ where the difficulty does not occur.

From (3.8) it can be seen that as soon as $|f_1(U)| \gg (X_s - X)$, W is a function of U alone, and a solution of (3.2) with the viscous terms retained may be found in the form

$$U = U_0(Y_1) + (X_s - X)U_1(Y_1) + O\{(X_s - X)^2\}$$

$$V - Q'(X)U = V_0(Y_1) + O(X_s - X) \qquad (3.11)$$

$$W = W_0(Y_1) + (X_s - X)W_1(Y_1) + O\{(X_s - X)^2\}$$

where $Y_1 = Y - Q(X)$. Here $U_0(Y_1)$, $W_0(Y_1)$ are functions of Y_1 satisfying $U_0 \to K^{-1/2}$, $W_0 \to -3/2\, kK^{-1/2}$ as $Y_1 \to \infty$, and $U_0 \to 0$, $W_0 \to \infty$ as $Y_1 \to -\infty$, and V_0, V_1, W_1 may be determined successively. This was also the situation in ref. 26 where, as here, the function Q(X), which is below shown to be large as $X \to X_s^-$, gives the position of the main part of the streamwise boundary layer.

The matching between (3.8) and (3.9) follows closely that in ref. 26. Since (3.6) is fully determined apart from β_1 in (3.7) and an arbitrary constant γ_1 at the n = 1 stage, both of which are expected to be determined by conditions for $X < X_s$, the matching serves merely to determine $f_1(U)$ for small U and to verify the consistency of the procedure. When U is small but W large, as occurs at the outer edge of the wall layer as was shown in ref. 26 by an examination of (3.6) for $\eta_1 \gg 1$, it follows from (3.9) that

$$W \sim U/[X_s - X + f_1(U)] \tag{3.12}$$

and matching with (3.6) as in ref. 26 leads to

$$f(U) = \frac{U}{2\overline{U}^{3/2}}\left[1 - \alpha_1\left(\frac{3}{2}\alpha_2 + 1\right)\frac{\log \overline{U}}{\overline{U}} + O\left(\frac{1}{\overline{U}}\right)\right] \tag{3.13}$$

where $\overline{U} = 4/3\ \alpha_1 \log \beta_1/U$. In ref. 26 it was possible to define a meaningful stream function for the inviscid flow that held for all Y. Here, however, this is not so but if we wish we may define ψ such that

$$\frac{\partial \psi}{\partial Y} = \frac{U}{W} \tag{3.14}$$

and then the match with (3.6) gives, again as in ref. 26,

$$\psi = (X_s - X)\left[Y + \frac{Y^2}{4\mu_1} + \frac{Y^3}{24\mu_1^2} + \frac{\alpha_1 \log \mu_1}{12\mu_1^{7/3}} Y^2 + O(\mu_1^{-7/3})\right] \tag{3.15}$$

when $U \ll 1$, $W \gg 1$, i.e. when $\eta_1 \gg 1$. It also follows from the form of U in (3.8) that in this region U itself is a function of ψ with

$$U = \psi\Psi^{3/4}\left[1 + \left(\frac{3\alpha_2}{4} - \frac{1}{4}\right)\frac{\alpha_1 \log \Psi}{\Psi} + O\left(\frac{1}{\Psi}\right)\right], \tag{3.16}$$

where $\Psi = 4/3[\alpha_1 \log(\ _1/\psi)]$, and that $f_1(U) = f(\psi)$ where

$$f(\psi) = \frac{\psi}{2\Psi^{3/4}}\left[1 - \left(\frac{3\alpha_2}{4} - \frac{1}{4}\right)\frac{\alpha_1 \log\Psi}{\Psi} + O\left(\frac{1}{\Psi}\right)\right] \tag{3.17}$$

The advantage of the formulation in terms of ψ is that Q(X) may be calculated as was the corresponding quantity in ref. 26. On the assumption that the inviscid flow contains no singularities other than as $U \to 0$, i.e. there is no value of Y at which $f_1(U)$ in (3.10) changes sign when $U = O(1)$, then the principal contribution to Q(X) comes from the inner part of the inviscid layer and

$$Q(X) = \frac{6}{7\alpha_1}\mu_1^{7/3}\left[1 - \frac{28\alpha_1}{9}\frac{\log \mu_1}{\mu_1^{4/3}} + O\left(\mu_1^{-4/3}\right)\right] \tag{3.18}$$

Thus the match appears to be consistent. If $K < 0$, i.e., $k > 0$ or $k < -2/3$, the procedure cannot be carried through as μ_1 then turns out to be negative and it is not possible to regard the situation as the termination of a boundary layer that exists for $X < X_s$. If $0 > k > -1/3$ it may be that an additional viscous layer is required in what we have termed the *inviscid region*. However, even in that situation the match between the wall layer and the inviscid region is satisfactory and the additional layer will affect only Q(X) in (3.18) and the main part of the streamwise boundary layer that is now centered on $Y = Q(X)$.

In the following section we shall make comparisons between the theory and a numerical integration at $k = -1/2$, but before doing so it is worth considering briefly the effect of suction on the present asymptotic theory since

suction is used to initiate this computation. The change in the boundary conditions required is that now in (3.3) $V = V_w$ where V_w is a given negative constant. The leading term of the expansion (3.6) is formally unaltered but the compatibility condition of ref. 26 is now dominated by V_w instead of by K so that instead of (3.7) we have

$$\eta_1 = \gamma\mu_1^{-1/3}, \quad \bar{\mu}_1^{1/3} - \bar{\alpha}_1\bar{\alpha}_2 \log(\bar{\mu}_1^{1/3} + \bar{\alpha}_1\bar{\alpha}_2) = \frac{\bar{\alpha}_1}{3} \log\left(\frac{\bar{\beta}_1}{X_s - X}\right) \tag{3.19}$$

where $\bar{\alpha}_1 = -2V_w\bar{\alpha}_1$, $\bar{\alpha}_2$ is a constant determined solely by the singularity and $\bar{\beta}_1$ a constant which depends on the history of the solution. The expansion (3.6) now proceeds in descending powers of $\bar{\mu}_1^{1/3}$: thus whether there is suction or not the appropriate powers of $\log[\bar{\beta}_1/(X_s-X)]$ are negative integers. If $V_w > 0$ the theory fails. It is possible that in this case an analysis similar to that carried out by Catherall, Stewartson and Williams[27] for the separation of a boundary layer with uniform external velocity and uniform injection will be relevant.

3.4 Comparison with the Numerical Solution When k = -1/2

The numerical solution when k = -1/2, some of whose principal properties are displayed in Fig. 3, may be used to illustrate our theory. We make the comparisons on the scaled quantities in (3.12) which are easily obtained from the numerical integration of (2.19) to (2.21). We define the longitudinal and azimuthal skin frictions by

$$\tau_X = \left.\frac{\partial U}{\partial Y}\right|_{y=0} \quad \text{and} \quad \tau_\phi = \left.\frac{\partial W}{\partial Y}\right|_{y=0} \tag{3.20}$$

respectively, and it then follows as in ref. 26 that

$$\zeta_1(X) = (\tau_\phi^{4/3} + \alpha_1\alpha_2)^{3\alpha_2/4} \exp\left(-\frac{3}{4\alpha_1}\tau_\phi^{4/3}\right) \tag{3.21}$$

should be close to $(X_s - X)/\beta_1$ as $X \to X_s$, and that

$$\theta_1(X) = \frac{\tau_X}{\tau_\phi}\left(1 + 0.266\tau_\phi^{-8/3}\right) \tag{3.22}$$

should be close to $X_s - X$. We may also compare W_{max} which is given by the formula of ref. 26 as

$$W_{max} = 2\tau_\phi^2\left\{1 - \frac{16\alpha_1}{3}\frac{\log\tau_\phi}{\tau_\phi^{4/3}} + O(\tau_\phi^{-4/3})\right\} \tag{3.23}$$

on identifying μ_1 with τ_ϕ, which is consistent with the order of accuracy of (3.23).

In Table 1 we present τ_ϕ, τ_X, $\zeta_1(X)$, $\theta_1(X)$ and in Table 2 present W_{max} computed from the differential equations and also from (3.23). For convenience we retain the abscissa as x and note the relationship $(x_s - x)/x_s \doteq (X_s - X)$ when $X_s - X$ is small. From $\zeta_1(X)$ we would infer that $x_s = 0.3786$ and $\beta_1 = 53.8$ while from $\theta_1(X)$ that $x_s = 0.3793$. The agreement between the two calculations of W_{max} is also satisfactory in view of the order of magnitude of the error in (3.23).

One comparison, possible in ref. 26, but not here because of the too rapid rise in the boundary-layer thickness as $x \to x_s^-$, is between the asymptotic estimate for the displacement thickness and the value computed from the differential equation. The significant function is

$$Q'(X) = K^{1/2} \lim_{Y\to\infty}\left\{V + \frac{3}{2}(k+1)YK^{-1/2}\right\} \tag{3.24}$$

Table 1. The Values of τ_ϕ, τ_X from the Numerical Integration and $\zeta_1(X)$, $\theta_1(X)$ from (3.21), (3.22)

x	τ_ϕ	τ_X	$\zeta_1(X)$	$\theta_1(X)$
0.20	2.202	0.826	0.01264	0.387
0.25	2.349	0.669	0.00853	0.293
0.30	2.564	0.478	0.00473	0.191
0.35	2.978	0.220	0.00148	0.0749
0.3562	3.074	0.180	0.00112	0.0595
0.3625	3.191	0.137	0.000796	0.0436
0.3656	3.272	0.116	0.000629	0.0357
0.3672	3.312	0.104	0.000559	0.0316
0.3687	3.366	0.0921	0.000476	0.0276
0.3703	3.419	0.0797	0.000406	0.0236
0.3719	3.492	0.0676	0.000328	0.0195

Table 2. The Values of W_{max} from the Numerical Integration and from (3.23), and of $Q'(X)$ from (3.25)

x	W_{max}	Eq.(3.23)	$Q'(X)$
0.20	2.082	1.784	9.44
0.25	2.345	2.463	13.28
0.30	2.842	3.130	22.25
0.35	4.264	4.905	66.04
0.3562	4.876	5.915	86.32
0.3625	5.327	6.081	122.11
0.3656	5.774	6.570	153.17
0.3672	6.050	6.823	175.24
0.3687	6.376	7.177	204.01
0.3703	6.749	7.534	245.54
0.3719	7.246	8.036	300.38

and according to our theory

$$Q'(X) = \frac{2\tau_\phi^2}{\tau_X}\left\{1 - \frac{4\alpha_1}{3}\frac{\log \tau_\phi}{\tau_\phi^{4/3}} + O(\tau_\phi^{-4/3})\right\} \quad \text{as} \quad \tau_\phi \to \infty \tag{3.25}$$

The values of $Q'(X)$ from this formula are also displayed in Table 2.

3.5 Computation of General Boundary Layers

As with our studies on leeward line of symmetry, a nonsimilar solution was produced near the vertex of the cone by assuming it to be permeable and

sucking fluid away from the boundary layer. Specifically we set

$$P = \begin{cases} +0.5 \exp[-(50x)^3] & 0 < x < 0.05 \\ 0 & x > 0.05 \end{cases} \tag{3.26}$$

at $\eta = 0$ for $0 \leq \phi \leq \pi$ where $\phi \sin \beta_c = \theta$ and $\beta_c = 10°$. Now a solution of (2.19) - (2.21) is possible at $x = 0$ by neglecting the derivatives with respect to x and solving the two-dimensional boundary-layer equations which result, using the standard box method and integrating from the windward line of symmetry $\phi = 0$. At each new station of x the integration is carried out in the same way with the suction velocity defined in (3.26) until at $x = 0.05$ it is switched off being then already extremely small. Further downstream the standard box method was modified as necessary by introducing the zig-zag box but it is not clear that much was achieved thereby. For the limit of accessibility of integrations from the windward side is virtually coincident with the vanishing of g'' at $\eta = 0$ and it is only when $g' < 0$ that the zig-zag box makes for a significant improvement. Calculations from the leeward line of symmetry are desirable to complete the accessibility line and would need the more sophisticated techniques of the zig-zag and characteristic boxes since g' changes sign across the boundary layer near $\phi = \pi$. However, certain difficulties emerged from the studies near $\phi = \pi$ which need to be overcome before this can be initiated. We shall refer to them below and hope to address them at some future date.

The first calculation carried out was for $k = -0.5$ where k is defined by (2.23). This value was chosen as being in the range when the leeside solution develops a singularity at a finite value of x but the semi-similar solution, valid in the limit $x \to \infty$, exists for all $\phi < \pi$ and implies a boundary-layer collision at $\phi = \pi$. The step length in x in the complete calculation varied from 0.005 in the suction regime to 0.025 when the solution was almost semisimilar ($x \to \infty$), in η was 0.1 and in ϕ varied from 10° near the windward line of symmetry to 0.2° right near the leeward line. The results were straightforward as expected except near the leeward line and deserve no further comment. In this neighborhood, however, an interesting nonuniformity developed which is illustrated in Fig. 4 where the computed values of f''_w are displayed as a function of ϕ, x. Three estimates of f''_w at $\phi = 180°$ are shown, one obtained by integrating with $\Delta\phi = 5°$, the second by integrating from $\phi = 175°$ with $\Delta\phi = 1°$ and the third by integrating from $\phi = 179°$ with $\Delta\phi = 0.2°$. All three differ substantially and, for $x < 0.375$, from the leeside line of symmetry solution although it could be argued that they are all consistent. The most likely explanation is that there is an eigenvalue attached to the leeside line of symmetry solution so that when $180-\phi$ is small

$$f = f_\ell(\eta, x) + A_n(180-\phi)^n f_{\ell n}(\eta, x) + \ldots \qquad (3.27)$$

where n is not an integer and A_n is arbitrary. We have not been able to pursue this possibility in detail but a preliminary inspection suggests that $n \zeta 0.2$. Some additional evidence in favor of a nonintegral eigenvalue is indirectly provided by Murdock's studies[18] on line-of-symmetry solutions but we should emphasize that none has been found to date. The consequences for an integration procedure starting from the leeside may be serious since A_n depends in some way on the rest of the solution and cannot be specified a

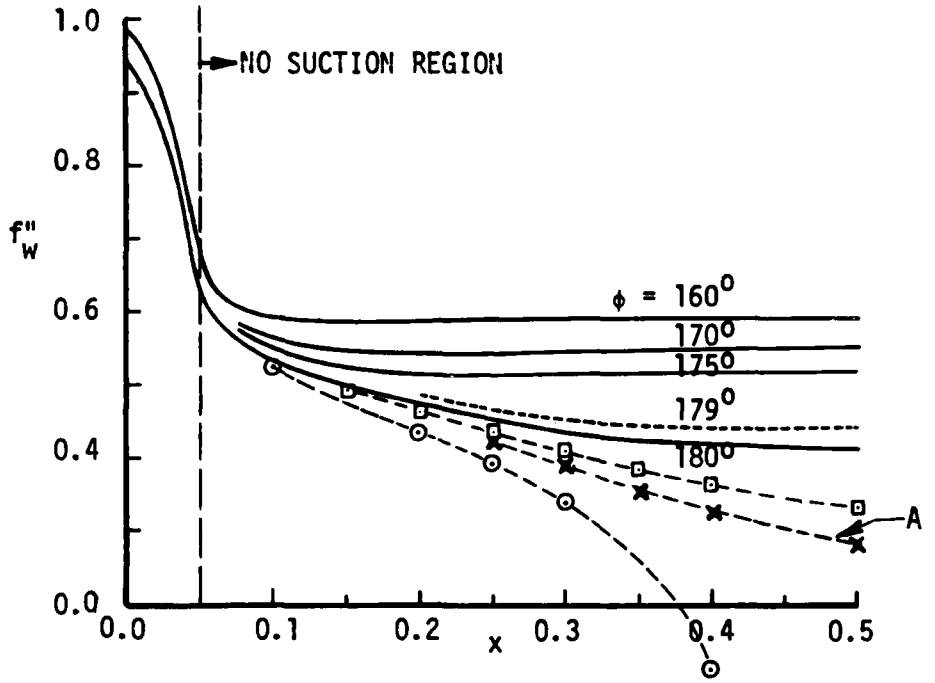

Fig. 4. Effect of varying step size in the circumferential direction on the wall shear parameter of the leeward line of symmetry, k = -0.50. The symbols o---o-- denote leeward solutions obtained from the line-of-symmetry equations. The solid lines (——) denote solutions obtained from the full equations with $\Delta\phi = 5^0$, the dashed lines those with $\Delta\phi = 1^0$ for $\phi > 175^0$, and the line denoted by A is obtained by taking $\Delta\phi = 0.2^0$ for $\phi > 179^0$.

priori. It is possible that A_n and n can be fixed when x is small but this remains to be investigated.

The implication of our analytic studies is that the cross-flow velocity is zero on the leeside line of symmetry for $x < x_s$ (=0.3793) and thereafter there is a collision phenomenon defined by g having a nonzero limit as $\phi \to \pi$. It follows that the cross-velocity, in the two boundary layers which spread around each side of the cone from the windward line of symmetry, are nonzero and equal in magnitude but opposite in sign when they reunite at the leeside. The consequence is that a jet of fluid is emitted from the boundary layers here although the present theory does not enable us to make any firm deductions about its subsequent fate.

Our numerical studies lend some support to the predictions of the analysis. For example, when $x < x_s$ the limit value of g_w'' as $\phi \to \pi^-$ is less than 10^{-5} in magnitude (typically it is 10^{-1} for $\phi < \pi$) and oscillates in sign. Within the limits of numerical error we may infer that it is zero at $\phi = \pi$. If $x < x_s$ the limit value of g_w'' soon becomes definitely positive, of order 10^{-4}, and seems to be approaching the value required by Fig. 2b as $x \to \infty$.

The next calculation was carried out for k = -0.75 when the leeside line-of-symmetry equations again have dual solutions and the semi-similar equations valid as $x \to \infty$, have solutions for all $|\phi| < \pi$ a collision occurring at $\phi = \pi$. The principal features of interest are again in the neighborhood of $\phi = \pi$. In Fig. 5 we display the variation of f''_w with x for various ϕ and we see that for $\phi \leq 170°$ the structure of f''_w is entirely reasonable, the limit solution being rapidly obtained as x increases once the suction is removed. For $\phi = 175°$, the smooth trend downwards of f''_w is disturbed and at the next station of ϕ, namely the leeside $\phi = 180°$, f_w increases and shows little sign of becoming constant as x increases.

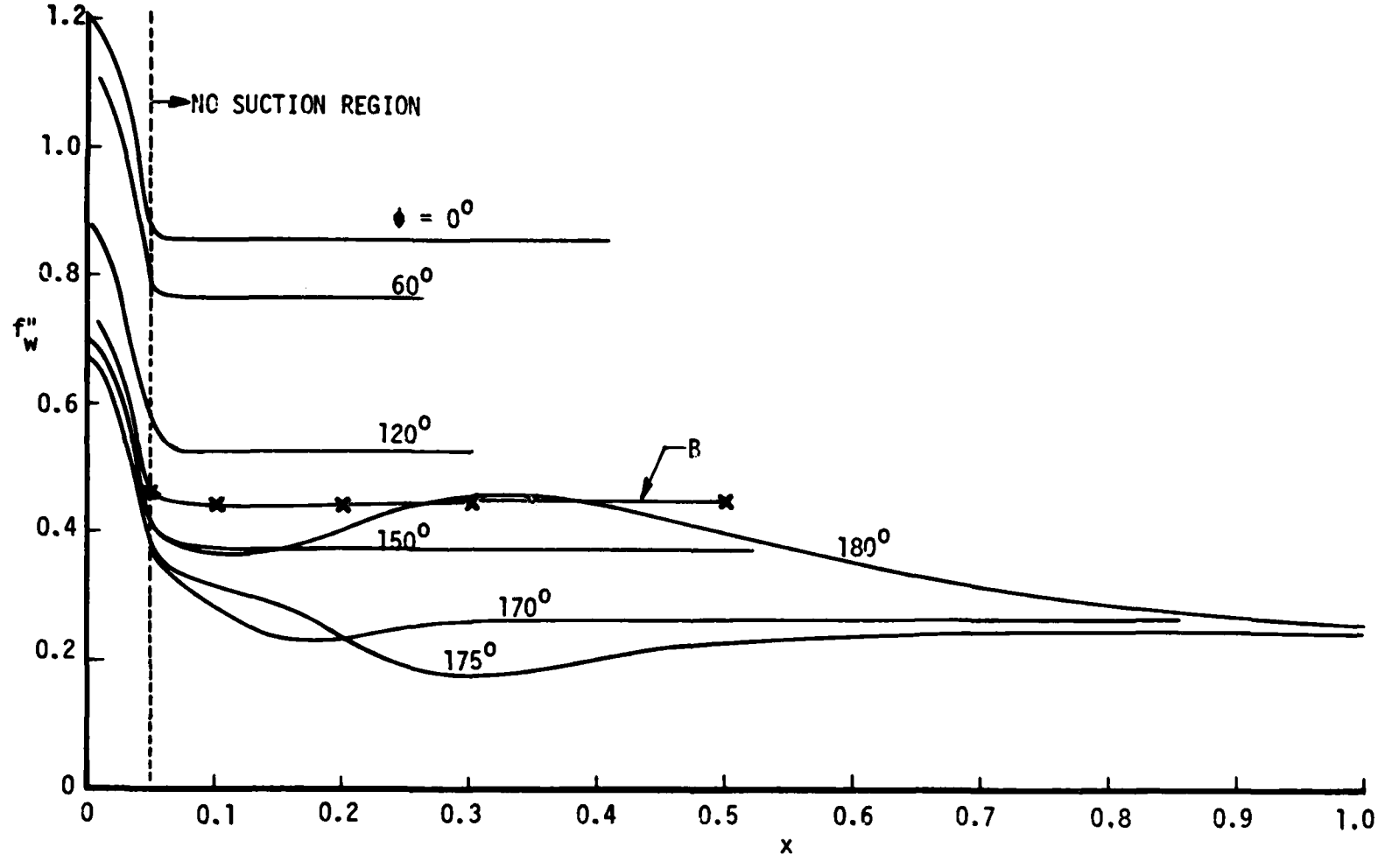

Fig. 5. Variation of wall shear parameter with x for various values of ϕ for k = -0.75. The line denoted by B is obtained from the leeside line-of-symmetry equations.

Moreover, there is a semi-similarity solution along $\phi = 180°$ which is quite different from the limit form as $\phi \to 180°$. It is possible that closer agreement between the two calculations will be obtained if $\Delta\phi$ is decreased substantially near $\phi = 180°$, and also that the leeside solution has an associated eigensolution at $k = -0.75$ as well as at $k = -0.50$.

The third calculation was carried out for $k = -0.82$ when the semi-similar solution valid as $x \to \infty$ separates at $\phi \simeq 170°$. Cooke examined such solutions[21] for $k \leq -1.33$ and concluded that they develop a singularity as the separation point $\phi = \phi_s$ is reached, but we see no evidence of it when $k = -0.82$ from the behavior of f''_w and g''_w. Even when the step length in ϕ is reduced to 1^0, behavior of g''_w shows no sign of the square-root behavior

$$g''_w \propto (\phi_s - \phi)^{1/2} \tag{3.28}$$

predicted by Brown's theory[28]. The integration of the general equations showed that even with the use of the zig-zag box, great care must be used near the separation line. Thus, after the suction is switched off, we uniformly took $\Delta x = 0.01$ but either chose $\Delta\phi = 5°$ or reduced it to $\Delta\phi = 1°$ for $\phi > 150^0$. In the first instance, the solution could be obtained right up to $\phi = 180°$ with largely believable data for $\phi > 165°$ even though $g''_w < 0$. Moreover, e_∞, the effective blowing velocity of the boundary layer, defined by

$$-e_\infty = \frac{3}{2}\int_0^\infty (1 - f')d\eta + x\frac{\partial}{\partial x}\int_0^\infty (1 - f')d\eta + \frac{w_e}{2u_e^2}\int_0^\infty (g' - w_e)d\eta$$

$$- \frac{1}{u_e}\frac{\partial}{\partial\theta}\int_0^\infty (g' - w_e)d\eta \tag{3.29}$$

shows little sign of irregular behavior in the separated region.

Once the step length $\Delta\phi$ is reduced to $1°$ a dramatic change takes place in the solution: g''_w changes sign at $x = 0.08$, $\phi = 168°$, for $x = 0.09$

the solution breaks down at $\phi = 168°$, and by $x = 0.120$ the separation line has been settled down to $\phi = 166°$. As with the semi-similarity solution, when $x = \infty$, g''_w shows little sign of any singular behavior but, on the other hand, e_∞ peaks up to 137 at $\phi = 167°$, $x = 0.100$. This last result is in marked contrast to the behavior for $\phi \leq 165°$ where it is less than 4.

The main conclusion from this integration is that unless care is taken, the boundary-layer equations will generate solutions where none should exist and moreover the effect of the boundary layer on the external flow, in the neighborhood of separation, will be diminished. Since we know from our studies of two-dimensional separation that it is important to have accurate estimation of the displacement thickness in order to carry out effective interaction studies, this conclusion is a matter of some concern. Of course, it may be that the effect is weaker in three-dimensions than in two but it would be premature to assume this at the present stage. It was hoped to use the calculation here to comment on the parabolic elliptic method for solving boundary-layer problems on cones. In this method diffusion terms in ϕ are added to the equations and the new set solved by the ADI procedure. In the event we cannot do this at present because we have not obtained the correct solution in any part of the integration domain $\phi > \phi_s$. A further study of the solution near the leeward line of symmetry seems called for in light of the present work to elucidate the role of the eigensolution and to mark out the remainder of the accessibility boundary possibly with the use of the characteristic box.

A final calculation was carried out to test our conclusions about separation. This was done at $k = -0.95$. Here breakdown first occurred in the suction region and by the end of this region separation was well established at $\phi = 153°$. Again there is little sign of a singularity in g''_w as separation

is approached and while a peak in e_ω was observed at $x = 0.05$, $\phi = 153°$. However, the magnitude of this peak is only 14 and much weaker than when $K = -0.82$. Comparative plots of the variation of e_ω with ϕ for different values of x are shown in Fig. 6.

3.6 Summary

We have shown that there is strong evidence that a singularity can and does develop in the integration of the boundary-layer equations on the leeward line of symmetry of a cone at incidence. Further we believe that there is convincing evidence that when it does occur it heralds the start of a collision pheomenon in which the boundary layers coming from the windward line of symmetry on the two sides of the cone have a nonzero cross-flow velocity distribution when they meet at the leeside line of symmetry. A full resolution of this phenomenon is not yet available and almost certainly will require consideration outside the scope of a hierarchical boundary-layer theory.

The formal conditions for the occurrence of the singularity were deduced by adapting the theory in ref. 26 for the singularity in the boundary layer on the inside line of symmetry of a curved pipe and are that $0 > k > -2/3$ whatever be the Mach number and prescribed wall temperature. However, it is known that similarity solutions of the governing equations exist when $k > k_1^*$ and $k_2^* > k > -1$ where $k_1^*(<0)$ and k_2^* depend on M_e and the wall temperature although $k_1^* > k_2^* > -2/3$. Our numerical solutions indicate that if the initial profile is arbitrary, these similarity solutions will appear as limits of more general solutions when $x \to \infty$ and that only if $k_2^* < k < k_1^*$ does the singularity occur.

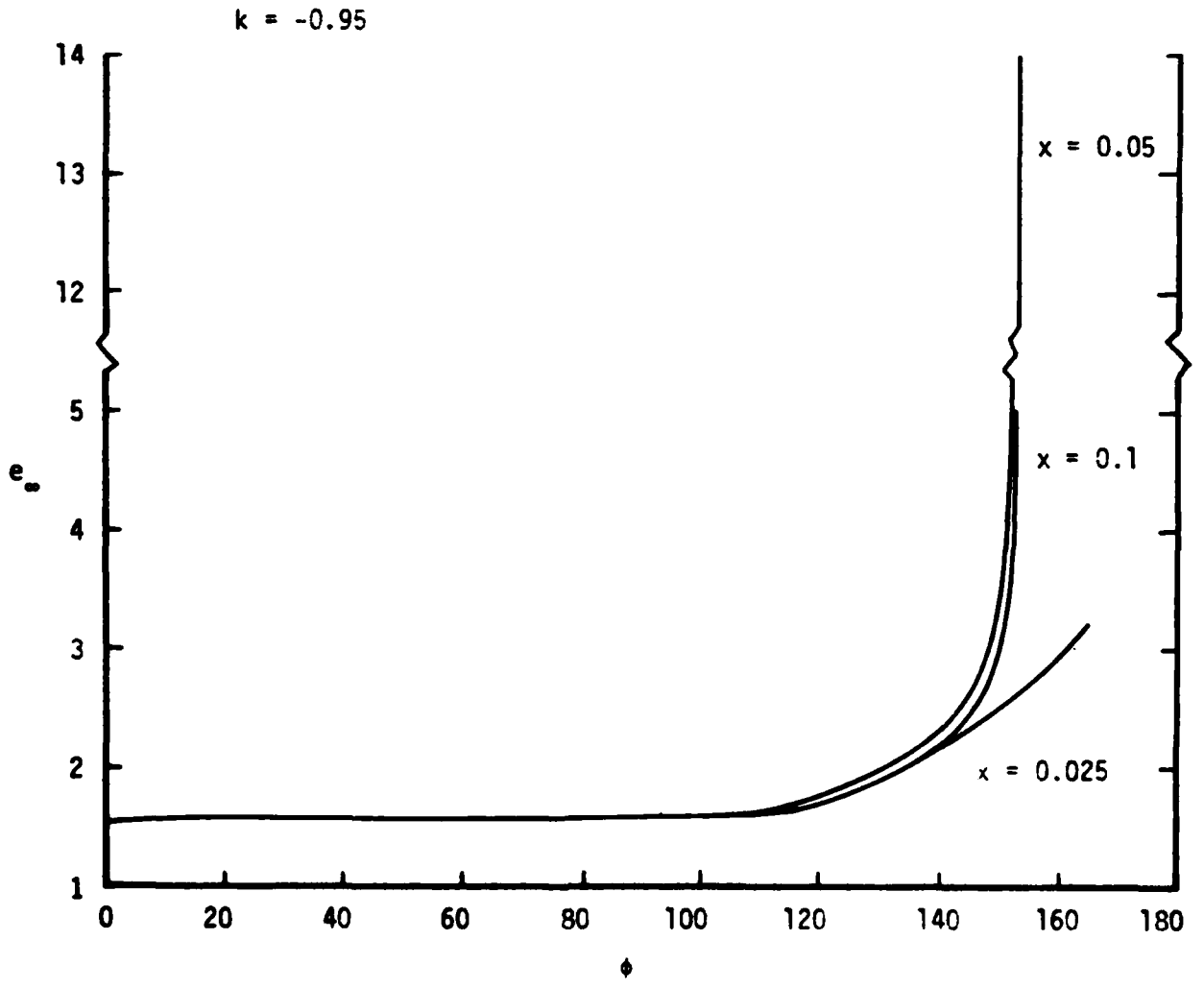

Fig. 6. Variation of e_∞, the reduced normal velocity at the outer edge of the boundary layer, with $\phi = \theta/\sin\beta_c$ for k = -0.95 and x = 0.025, 0.05, 0.1. It is noted that similarity is virtually achieved as soon as the suction is removed.

4.0 REFERENCES

1. Cebeci, T., Khattab, A.A. and Stewartson, K.: On Nose Separation. J. Fluid Mech. 97, 1980, pp. 435-454.

2. Cebeci, T., Khattabh, A.A. and Stewartson, K.: Three-Dimensional Laminar Boundary Layers and the Ok of Accessibility. J. Fluid Mech., 107, 1981, pp. 57-87.

3. Keller, H.B.: A New Difference Scheme for Parabolic Problems. In Numerical Solution of Partial-Differential Equations, Bramble, J. (ed.) Vol. II, Academic Press:New York, 1970.

4. Cebeci, T.: The Laminar Boundary Layer on a Circular Cylinder Started Impulsively from Rest. J. Comp. Phys., 31, 1979, pp. 153-173.

5. Cebeci, T. and Stewartson, K.: Unpublished work, 1977.

6. Cebeci, T., Stewartson, K. and Williams, P.G.: Separation and Reattachment Near the Leading Edge of a Thin Airfoil at Incidence. AGARD Symp. Computation of Viscous-Inviscid Interacting Flows, Colo. Springs, 1980.

7. Stewartson, K., Smith, F.T. and Kaups, K.: On Marginal Separation. To appear in Studies in Applied Math, 1982.

8. Gault, D.E.: An Experimental Investigation of Regions of Separated Laminar Flow. NACA TN3505, 1955.

9. Cebeci, T.: Recent Progress in the Calculation of Interacting Flows. To be presented at the DEA Meeting held in Gottingen, Germany, 1981.

10. Cebeci, T. and Stewartson, K.: On the Calculation of Separation Bubbles. Paper in preparation.

11. Schiff, L.B. and Steger, J.L.: Numerical Simulation of Steady Supersonic Viscous Flow. AIAA J., 18, 12, 1980, pp. 1421-1430.

12. Sturek, W.B., Mylin, D.C. and Heavey, K.R.: Computational Study of the Flow Over Boattailed Shell at Supersonic Speeds. Paper presented at the DEA Meeting held in Gottingen, Germany, 1981.

13. Moore, F.K.: Laminar Boundary Layer on Cone in Supersonic Flow at Large Angle of Attack. NACA Rept. No. 1132, 1953.

14. Sims, J.L.: Tables for Supersonic Flow Around Right Circular Cones at Small Angle of Attack. NASA SP-3007, 1964.

15. Bradshaw, P., Cebeci, T. and Whitelaw, J.H.: Engineering Calculation Methods for Turbulent Flows. Academic Press, New York, 1981.

16. Cheng, H.K.: The Shock Layer Concept and Three-Dimensional Hypersonic Boundary Layers. Cornell Aero. Lab. Rept. AF-1285-A-3, 1961.

17. Roux, B.: Supersonic Laminar Boundary Layer Near the Plane of Symmetry of a Cone at Incidence. J. Fluid Mech., 51, 1972, pp. 665-678.

18. Murdock, J.W.: The Solution of Sharp-Cone Boundary-Layer Equations in the Plane of Symmetry. J. Fluid Mech., 54, 1972, pp. 665-678.

19. Wu, P. and Libby, P.A.: Laminar Boundary Layer on a Cone Near a Plane of Symmetry. AIAA J., 11, 1973, pp. 326-333.

20. Rubin, S.G., Lin, T.C. and Tarulli, F.: Symmetry Plane Viscous Layer on a Sharp Cone. AIAA J., 15, 1977, pp. 204-211.

21. Cooke, J.C.: Supersonic Laminar Boundary Layers on Cones. RAE Farnborough Rept. No. 66347, 1964.

22. Boericke, R.R.: The Laminar Boundary Layer on a Cone at Incidence in Supersonic Flow. AIAA J., 9, 1971, pp. 462-468.

23. Tarulli, F.: The Boundary Layer on a Cone at Angle of Attack. M.S. Thesis, Polytechnic Inst. of New York, 1974.

24. Dwyer, H.A.: Boundary Layer on a Hypersonic Sharp Cone at Small Angle of Attack. AIAA J., 9, 1971, pp. 277-284.

25. Stewartson, K., Cebeci,T. and Chang, K.C.: A Boundary-Layer Collision in a Curved Duct. Quart. J. Mech. and Appl. Math., 33, 1980, pp. 59-75.

26. Stewartson, K. and Simpson, C.J.: On a Singularity Initiating a Boundary-Layer Collision. To appear in Quart. J. Mech. and Appl. Math., 1981.

27. Catherall, D., Stewartson, K. and Williams, P.G.: Viscous Flow Past a Flat Plate with Uniform Injection. Proc. Roy. Soc., Lond. A 284, 1965, pp. 370-396.

28. Brown, S.N.: Singularities Associated with Separating Boundary Layers. Phil. Trans. Roy. Soc. Lond. A 257, 1965, pp. 409-444.